

Role of Radical Species in Salicylaldiminato Ni(II) Mediated Polymer Chain Growth: A Case Study for the Migratory Insertion Polymerization of Ethylene in the Presence of Methyl Methacrylate

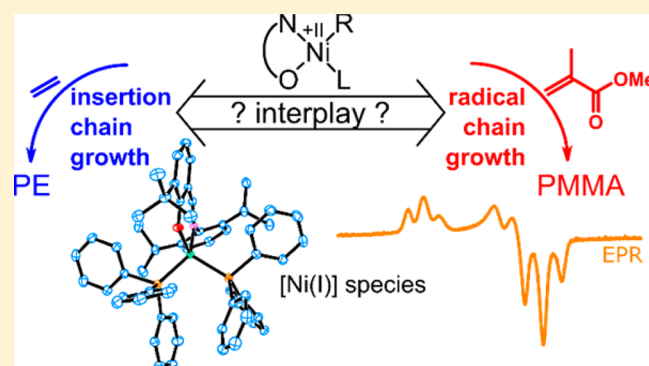
Franz Ölscher,[†] Inigo Göttker-Schnetmann,[†] Vincent Monteil,[‡] and Stefan Mecking^{*,†}

[†]Chair of Chemical Materials Science, Department of Chemistry, University of Konstanz, D-78464 Konstanz, Germany

[‡]Université de Lyon, Univ. Lyon 1, CPE Lyon, CNRS UMR 5265 Laboratoire de Chimie Catalyse Polymères et Procédés (C2P2), LCPP team Bat 308F, 43 Bd du 11 novembre 1918, F-69616 Villeurbanne, France

S Supporting Information

ABSTRACT: To date, an inconclusive and partially contradictory picture exists on the behavior of neutral Ni(II) insertion polymerization catalysts toward methyl methacrylate (MMA). We shed light on this issue by a combination of comprehensive mechanistic NMR and EPR studies, isolation of a key Ni(I) intermediate, and pressure reactor studies with ethylene and MMA, followed by detailed polymer analysis. An interlocking mechanistic picture of an insertion and a free radical polymerization is revealed. Both polymerizations run simultaneously (25 bar ethylene, neat MMA, 70 °C); however, the chain growth cycles are independent of each other, and therefore exclusively a physical mixture of homo-PE and homo-PMMA is obtained. A Ni–C bond cleavage was excluded as a free radical source. Rather a homolytic P–C bond cleavage in the labile aryl phosphine ligand and the reaction of low-valent Ni(0/I) species with specific iodo substituted N[∧]O (Ar–I) ligands were shown to initiate radical MMA polymerizations. Several reductive elimination decomposition pathways of catalyst precursor or active intermediates were shown to form low-valent Ni species. One of those pathways is a bimolecular reductive coupling via intermediate (N[∧]O)Ni(I) formation. These intermediate Ni(I) species can be prevented from ultimate decomposition by capturing with organic radical sources, forming insertion polymerization active [(N[∧]O)Ni(II)–R] species and prolonging the ethylene polymerization activity.



INTRODUCTION

While catalytic polymerizations of ethylene (E) and propylene are applied on a very large scale, an incorporation of polar vinyl monomers in such reactions is challenging. The common early transition metal catalysts employed are deactivated by polar compounds due to their high oxophilicity. This problem can be addressed by late transition metal catalysts that are less oxophilic and more functional group tolerant.¹ For example, a copolymerization of ethylene with acrylates was achieved with Brookhart's cationic α -diimine Pd(II) complexes. As a result of a chain walking mechanism, highly branched polyethylene is formed with the acrylate-derived repeat units located at the ends of branches preferentially.² By contrast, neutral κ^2 -phosphine-sulfonato Pd(II) complexes form linear copolymers of ethylene and acrylates.³ These catalysts⁴ are compatible with a range of polar vinyl monomers, including difficult candidates like acrylonitrile,⁵ vinyl acetate,⁶ and acrylic acid.⁷ High incorporations of methyl acrylate (MA) of up to 52 mol % were achieved. In the absence of ethylene, MA is homopolymerized by an insertion mechanism.⁸ By contrast, methyl methacrylate (MMA) is not incorporated by these catalysts.⁹

Unique catalyst systems in the general context of functional group tolerant polymerizations are κ^2 -N[∧]O-salicylaldiminato Ni(II) complexes.¹⁰ Remarkably, these are tolerant toward polymerizations in aqueous media.¹¹ Additionally, copolymerization of ethylene with substituted norbornenes or α -olefins, respectively, with a functional group in a remote position to the monomers' double bond have been reported.¹² Concerning fundamental monomers, like acrylates, Grubbs et al. reported that no polymers are formed in attempted copolymerizations of MA with ethylene applying salicylaldiminato Ni(II) complexes.¹³ Mechanistic studies provide an explanation for this finding. It has been shown that MA inserts into the Ni–C bond of [Ni–Ph]¹⁴ or [Ni–Me]¹⁵ complexes and also into reactive [Ni–H]¹⁵ species. However, further migratory chain growth is hindered due to chelate formation by the ester group of the inserted MA and β -H elimination occurs instead. The resulting [Ni–H] species reacts with the residual MA insertion product in a bimolecular elimination at temperatures ≥ 0 °C, resulting in

Received: October 22, 2015

Published: November 16, 2015

formation of saturated organic substrate and irreversible deactivation of the catalyst ($[\text{Ni}-\text{H}] + [\text{Ni}-\text{alkyl}] \rightarrow \text{H}-\text{alkyl} + \text{“Ni species”}$).^{15,16}

However, repetitive reports on the formation of polymers containing incorporated methyl methacrylate (MMA) with similar catalysts generate an inconclusive and partially contradictory picture. [Bis(β -ketoiminato)Ni(II)]/MAO systems were used for homopolymerizations of MMA. Here, a radical mechanism was proposed, involving a reversible Ni–C homolytic bond cleavage.¹⁷ Furthermore, the efficient copolymerization of ethylene and MMA mediated by [(β -ketoiminato)Ni(II)Ph(PPh₃)]/MAO systems was reported, claiming an insertion mechanism pathway.¹⁸ A similar approach using bimolecular salicylaldiminato N[^]O Ni(II) complexes to copolymerize ethylene and MMA via migratory insertion was reported; however, some results were not reproducible.¹⁹ In addition, a novel approach for the simultaneous polymerization of ethylene with MMA was described, combining a migratory insertion mechanism for ethylene and a radical mechanism for MMA, resulting in block copolymers.²⁰ Neutral [(N[^]O)_{iPr,I-1}Ni(II)Ph(PPh₃)] and [(κ^2 -phosphineenolate)Ni(II)Ph(PPh₃)] catalyst precursors were shown to be active for both types of polymerization mechanisms, with a postulated reversible homolytic Ni–C bond cleavage as transfer reaction between insertion and radical polymerization. Addition of PPh₃ to the nickel complexes promotes free radical MMA homopolymerizations and influences the MMA content in simultaneous polymerizations of ethylene with MMA.

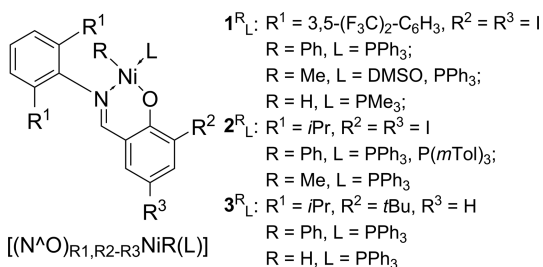
This mixed picture indicated that an elucidation of underlying reactions is of general interest to reveal relevant pathways not recognized to date in polar monomer polymerizations. We now report possible formation pathways and multiple roles of radicals in Ni(II) catalyzed polymerizations, as concluded from reactivities of intermediates observed under NMR and pressure reactor conditions and from detailed analysis of formed polymers.

RESULTS AND DISCUSSION

General Considerations. Various systems containing Ni(II) complexes have been shown to promote the simultaneous polymerization of ethylene and polar vinyl monomers.^{17,18,20,21} In our present study, we have focused on polymerizations of ethylene in the presence of MMA using neutral (N[^]O) salicylaldiminato Ni(II) aryl-phosphine complexes. For these systems, detailed mechanistic studies on the reaction of ethylene¹⁶ and MA^{14,15} have been reported previously (vide supra).

We have employed a number of different (N[^]O) Ni(II) complexes (Chart 1): Complexes with ligand (N[^]O)_{CF,I-1}⁻ (**1**^R)

Chart 1. General Notation of (N[^]O)Ni(II)R(L) Complexes Used in This Study



were selected for their robustness and high activity in ethylene polymerizations,^{11,22} and (N[^]O)_{iPr,I-1}⁻ was chosen because the corresponding phenyl PPh₃ complex (**2**^{Ph}_{PPh₃}) was described to mediate insertion and radical polymerizations.²⁰ Furthermore, complexes with ligand (N[^]O)_{iPr,tBu-H}⁻ (**3**^R_L) do not contain iodo substituents on the salicylaldehyde (R^2 and R^3 in **1** and **2**), which allows the determination of a specific influence of Ar–I functionalities. Besides [Ni–Ph] complexes as most common polymerization catalyst precursors, we used [Ni–Me] complexes as a closer mimic of the growing [Ni–alkyl] species in the ethylene polymerization. Additionally, [Ni–H] complexes were applied in this study because they are reactive intermediates formed after β -H elimination during insertion polymerization. In addition to phosphines, which were reported to promote the radical polymerization process,²⁰ dimethyl sulfoxide (DMSO) was used as a weakly coordinating ligand, enabling insertion reactions into the [Ni–C] moiety at milder conditions (for details, see Supporting Information).

Reactivity of Different Ni(II)-Catalyst Precursors toward MMA. Leblanc et al. reported that free radical MMA polymerizations occur in the presence of [(N[^]O)_{iPr,I-1}Ni(II)Ph(PPh₃)] (**2**^{Ph}_{PPh₃}), which are promoted by additional PPh₃.²⁰ However, the role of PPh₃ remained unclear. Herein, we provide further insights by performing homopolymerizations of MMA, labeling experiments, and detailed polymer analysis.

Homopolymerization of MMA Initiated with [(N[^]O)Ni(II)-R(PPh₃)] Complexes. To elucidate the effect of the salicylaldiminato ligand's substitution pattern and additional phosphine in [Ni] initiated MMA homopolymerizations, [(N[^]O)_{CF,I-1}NiPh(PPh₃)] (**1**^{Ph}_{PPh₃}) and [(N[^]O)_{iPr,tBu-H}NiPh(PPh₃)] (**3**^{Ph}_{PPh₃}) were reacted in neat MMA at 70 °C with different concentrations of PPh₃. A significant decrease in molecular weights was observed with increasing concentration of PPh₃ (Table 1, entries 1–3).

Table 1. MMA Homopolymerizations Initiated with Complexes **1^{Ph}_{PPh₃}, **1**^{Me}_{DMSO} and **3**^{Ph}_{PPh₃} with or without Additional PPh₃^a**

entry	complex	equiv add.	yield, %	M_w^b 10 ³ g·mol ⁻¹	chains/[Ni] ^c
1	1 ^{Ph} _{PPh₃}		2.8	803	0.05
2	1 ^{Ph} _{PPh₃}	3PPh ₃	6.2	610	0.14
3	1 ^{Ph} _{PPh₃}	5PPh ₃	6.8	463	0.26
4	1 ^{Me} _{DMSO}	3PPh ₃	7.2	563	0.21
5	3 ^{Ph} _{PPh₃}		1.1	270	0.06
6	3 ^{Ph} _{PPh₃}	3PPh ₃	1.8	251	0.10

^aReaction conditions: 70 °C, neat MMA, $c([\text{Ni}]) = 0.5 \text{ mmol}\cdot\text{L}^{-1}$. Details see Supporting Information. ^bDetermined by SEC (40 °C, THF) vs PS standards. ^cCalculated by $m(\text{PMMA})/[M_n(\text{PMMA})n([\text{Ni}])]$.

This observation can be rationalized by a higher steady state concentration of free radicals and therefore a higher rate of bimolecular termination reactions of the growing radical polymeric species (by radical recombination or disproportionation).²³ An accurate measure for the efficiency of the polymerization initiation reaction is the amount of PMMA chains formed per Ni center (chains/[Ni]). In the absence of additional PPh₃, 0.05 chains/[Ni] were formed with complex [(N[^]O)_{CF,I-1}NiPh(PPh₃)], while addition of 3 or 5 equiv of PPh₃ increased the chains/[Ni] ratio to 0.14 and 0.26, respectively. Similarly, for [(N[^]O)_{iPr,tBu-H}NiPh(PPh₃)], a ratio of 0.06 chains/[Ni] was obtained, which increased to 0.10 with 3 equiv of PPh₃

(Table 1, entries 5 and 6). This already points out a crucial role of the phosphine for the generation of free radicals. Beyond [Ni–Ph] complexes, a [Ni–Me] species ($1_{\text{DMSO}}^{\text{Me}}$ with 3 equiv of PPh_3), as a model compound for the growing [Ni–PE] species in ethylene polymerization, was shown to initiate radical MMA polymerizations, enabling comparable yields, molecular weights, and chains/[Ni] ratios (Table 1, entry 2 vs 4) and resembling similar kinetic polymerization behavior as the corresponding [Ni–Ph] complexes (Figure S16, red vs blue).

In addition to the effect of ligand substitution and the influence of additional phosphine, we investigated the effect of the concentration of initially supplied $[(\text{N}^{\wedge}\text{O})\text{Ni}(\text{II})\text{R}(\text{L})]$ on the efficiency of radical MMA polymerizations. This can give valuable insights into the initiation reaction, for example, if a key reaction step herein is mononuclear or bimolecular. To this end, $[(\text{N}^{\wedge}\text{O})_{i\text{Pr},1-\text{I}}\text{NiPh}(\text{PPh}_3)]$ ($2_{\text{PPh}_3}^{\text{Ph}}$), which was previously described to be an efficient radical polymerization initiator,²⁰ was reacted at different [Ni] concentrations with MMA (Table 2).

Table 2. MMA Homopolymerizations Initiated with Complex $2_{\text{PPh}_3}^{\text{Ph}}$ with Additional 3 equiv of PPh_3 in Dependency of the [Ni] Concentration^a

entry	complex	$c([\text{Ni}])$, $\text{mmol}\cdot\text{L}^{-1}$	yield, %	M_n^b , 10^3 g·mol ⁻¹	chains/ [Ni] ^c
1	$2_{\text{PPh}_3}^{\text{Ph}}$	0.5	4.3	321	0.18
2	$2_{\text{PPh}_3}^{\text{Ph}}$	4.1	16.0	35	0.63
3	$2_{\text{PPh}_3}^{\text{Ph}}$	8.4	27.1	12	1.52

^aReaction conditions: 3 equiv of PPh_3 , 70 °C, $c(\text{MMA}) = 9.389$ M for entry 1 and 5.633 M for entries 2 and 3, with toluene as a solvent. ^bDetermined by SEC (40 °C, THF) vs PS standards. ^cCalculated by $m(\text{PMMA})/[M_n(\text{PMMA})n([\text{Ni}])]$.

When the initial concentration of $2_{\text{PPh}_3}^{\text{Ph}}$ was raised from 0.5 to 4.1 and finally to 8.4 $\text{mmol}\cdot\text{L}^{-1}$, a significant increase in the amount of PMMA chains per [Ni] center (0.18, 0.63, and 1.52, respectively) was observed. That is, the radical polymerization initiation efficiency depends on the initial [Ni] concentration. This suggests a radical initiation process, which includes a reaction step involving more than one [Ni] center.

In analogy to, for example, cobalt mediated radical polymerizations,²⁴ one could expect a reversible trapping of the free radical PMMA chains by [Ni] species formed during polymerization. However, for $1_{\text{PPh}_3}^{\text{Ph}}$ and $2_{\text{PPh}_3}^{\text{Ph}}$ (with addition of PPh_3), a plot of $M_n(\text{PMMA})$ vs conversion is not linear, and polydispersities (M_w/M_n) are in the range of 2–5 (Figure S17). This indicates that no controlled polymerization was operative here.

The MMA homopolymerizations revealed that complexes $1_{\text{PPh}_3}^{\text{Ph}}$, $2_{\text{PPh}_3}^{\text{Ph}}$, and $3_{\text{PPh}_3}^{\text{Ph}}$ effectively promote radical MMA polymerizations, with a strong dependency on the phosphine and the initial [Ni] concentration. However, the nature of the initiating organic radicals remains unclear. Therefore, the PMMA polymers formed were studied in more detail to provide insights into the initiation process.

Microstructure and End Group Analysis of PMMA Homopolymers. According to literature reports,²⁰ a radical polymerization mechanism is active in the aforementioned polymerizations. This is confirmed, because PMMA homopolymers obtained by initiation with Ni(II) precursors show glass transition temperatures (T_g 's) of ca. 124 °C and are slightly syndio enriched (about 60% rr). This agrees with free radically

polymerized PMMA initiated with the radical initiator azo-bis(isobutyronitrile) (AIBN), applying similar reaction conditions (Figure S18–21). In addition, unsaturated end groups were detected by ¹H NMR spectroscopy (5.45 and 6.15 ppm in CD_2Cl_2 , Figure 1), which were formed via a bimolecular disproportionation reaction of two radical PMMA polymeryl chains.²³

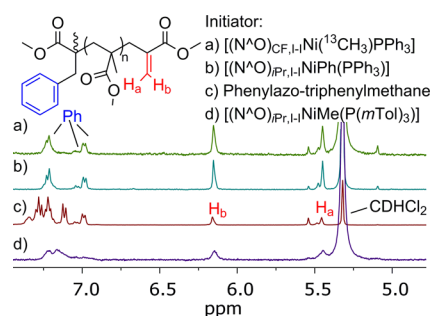


Figure 1. ¹H NMR spectra (400 MHz, CD_2Cl_2 , RT) of the olefinic and aromatic region of PMMA initiated with $1_{\text{PPh}_3}^{13\text{CH}_3}$ (a), $2_{\text{PPh}_3}^{\text{Ph}}$ (b), phenylazo-triphenylmethane (c), and $2_{\text{P}(m\text{Tol})_3}^{\text{Me}}$ (d). Details see Table S3.

To gain further insights into the initiation process, $^{13}\text{CH}_3$ labeled $1_{\text{PPh}_3}^{13\text{CH}_3}$ was employed as an initiator (60 °C, 3 equiv of PPh_3). The PMMA formed by initiation with $1_{\text{PPh}_3}^{13\text{CH}_3}$ should contain a ^{13}C labeled end group if the release of an organic free radical occurs by homolytic Ni–C bond cleavage after insertion of MMA into the Ni–C bond or directly from the [Ni–Me] precursor. However, no $^{13}\text{CH}_3$ label incorporation was detected by ^{13}C NMR spectroscopy in the PMMA formed ($M_{n,\text{NMR}} = 30 \times 10^3$ g/mol, Figure S22; quantification of products, see Supporting Information).²⁵ Therefore, both anticipated pathways for the initiation of the radical MMA polymerization, homolytic Ni–C bond cleavage of an MMA insertion product or the [Ni–Me] precursor, can be excluded. This also indicates that in the simultaneous polymerization of ethylene and MMA the alkyl moiety at the Ni center (e.g., PE polymeryl) is unlikely to initiate free radical MMA chain growth. This precludes the formation of PE-*block*-PMMA polymers via a simple homolytic Ni–C bond cleavage in [Ni–PE/alkyl] complexes.

Surprisingly, in the ¹H NMR spectrum of the PMMA formed by initiation with $1_{\text{PPh}_3}^{13\text{CH}_3}$, aromatic end groups were clearly identified (0.20 equiv with respect to H_b , Figure 1a). The same end groups could be identified when $2_{\text{PPh}_3}^{\text{Ph}}$ with 3 equiv of PPh_3 (0.25 equiv with respect to H_b , Figure 1b) or phenylazo-triphenylmethane (PAT) as a phenyl radical source (Figure 1c) were used as initiators. The assignment of phenyl end groups was further confirmed by matrix-assisted laser desorption/ionization time-of-flight mass spectroscopy (MALDI-TOF MS, Figure S66), and the ¹H NMR spectrum is in agreement with reported resonances for phenyl terminated PMMA.²⁶ Since PPh_3 is the sole phenyl source in $1_{\text{PPh}_3}^{13\text{CH}_3}$, the aryl end group of the resulting PMMA must originate from the phosphine compound. This was further confirmed by using $\text{P}(m\text{Tol})_3$ as a phosphine ligand in the initiator complex ($2_{\text{P}(m\text{Tol})_3}^{\text{Me}}$), indeed resulting in different ¹H NMR resonances of the aromatic end groups in the PMMA obtained from MMA homopolymerization (Figure 1d). Possible pathways to this end group formation are discussed later on in the section on sources of organic free radicals.

Reactivity of MMA toward Insertion Chain Growth Species. In the previous section, it was shown that the initiation

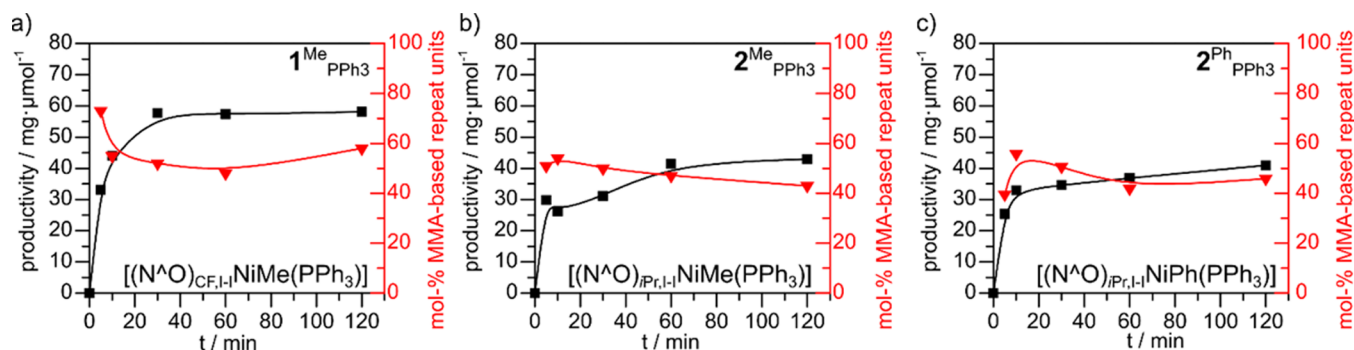


Figure 2. Time dependent plots of the overall productivity ($\text{mg}(\text{polymer})/\mu\text{mol}([\text{Ni}])$, \blacksquare , left axis), together with mol % MMA-based repeat units (\blacktriangledown , right axis) for the simultaneous polymerization of ethylene and MMA with complexes $1^{\text{Me}}_{\text{PPh}_3}$ (a), $2^{\text{Me}}_{\text{PPh}_3}$ (b), and $2^{\text{Ph}}_{\text{PPh}_3}$ (c). The lines were included as guidance for the eye. Reaction conditions: 70 °C, 3 equiv of PPh_3 , 50 mL of MMA, 25 bar of E. For details and additional data, see [Supporting Information](#).

of radical MMA polymerizations can be effectively initiated with $[(\text{N}^{\wedge}\text{O})\text{Ni}(\text{II})\text{R}(\text{PPh}_3)]$ complexes. In addition, these complexes are known as highly active catalyst precursors for ethylene insertion polymerization,²² and even simultaneous insertion and radical polymerizations were reported.²⁰ However, the results of the aforementioned homopolymerizations of MMA, do not allow a prediction of the nature of the polymers forming during insertion polymerization of ethylene in the presence of MMA. Different scenarios are conceivable, depending on the interaction of both polymerization modes: Statistical or block copolymers could be formed, or without any interaction, the formation of homo-PE and homo-PMMA mixtures would be anticipated. Therefore, we conducted insertion polymerizations of ethylene mediated by $[(\text{N}^{\wedge}\text{O})\text{Ni}(\text{II})\text{R}(\text{PPh}_3)]$ complexes in the presence of MMA and analyzed the polymers carefully.

Polymerization of Ethylene in the Presence of MMA. To provide kinetic insights, time dependent polymerizations with $1^{\text{Me}}_{\text{PPh}_3}$, $2^{\text{Me}}_{\text{PPh}_3}$, and $2^{\text{Ph}}_{\text{PPh}_3}$ with an additional 3 equiv of PPh_3 at 70 °C and 25 bar of ethylene were carried out in neat MMA (Figure 2). In every case, the resulting polymer product contained an almost equal amount of repeat units from ethylene and MMA. Generally, a reduced productivity in the insertion polymerization of ethylene was observed compared with previously described polymerizations in a noncoordinating solvent such as toluene.²² This can be accounted for by the coordination of additional PPh_3 or coordination of the ester group of the MMA solvent to a vacant coordination site on the Ni center, hindering the coordination of ethylene. Complex $1^{\text{Me}}_{\text{PPh}_3}$ was almost twice as productive as $2^{\text{R}}_{\text{PPh}_3}$ (R = Me, Ph) regarding the overall productivity (Figure 2, panel a vs b and c). The mol % content of MMA-based repeat units in the polymer product for all complexes evolved similarly over time (Figure 2, red). Most of the MMA was polymerized on the same time scale in which the insertion polymerization was mainly active; after ca. 40 min, the mol % MMA content in the product mixture decreased slightly (ethylene polymerization was more productive in comparison). No significant further conversion was observed for $1^{\text{Me}}_{\text{PPh}_3}$ after ca. 40 min (Figure 2a) and for $2^{\text{Ph}}_{\text{PPh}_3}$ after ca. 20 min (Figure 2b) in the presence of ethylene, while in homopolymerizations of MMA, significant further conversion was observed until 300 min for $1^{\text{Ph}}_{\text{PPh}_3}$ and up to 200 min for $2^{\text{Ph}}_{\text{PPh}_3}$ (Figure S16). Therefore, we conclude that in the presence of ethylene, the free radical polymerization of MMA proceeds much faster. A further indication for a faster and more efficient generation of free radicals in the presence of ethylene is the ratio of PMMA chains

formed per [Ni] center (details, see [Supporting Information](#)). Even though a lower initial [Ni] concentration was supplied in simultaneous ethylene and MMA polymerizations in comparison to the polymerization of MMA alone, a substantially higher PMMA chains per [Ni] center ratio of 0.35 was already established after 5 min. In polymerizations of MMA alone under similar conditions, such high ratios were not reached even after 2 h of reaction time (Table S2). Apparently, the presence of ethylene seems to accelerate the generation of free radicals.

The progress of initiation of the ethylene polymerization was studied by using ^{13}C labeled [Ni–Me] and [Ni–Ph] catalyst precursors, which introduce a detectable and quantifiable $^{13}\text{CH}_3$ or phenyl group at the PE chain end. Both catalyst precursors, $2^{\text{Me}}_{\text{PPh}_3}$ and $2^{\text{Ph}}_{\text{PPh}_3}$ (Table S6, entries 2 vs 5), were activated by ethylene to ca. 50% after 10 min; therefore, the activation rate by ethylene seems to be similar for the [Ni–Me] and [Ni–Ph] complexes here. The extent of activation eventually further increased up to 62% after 120 min for complex $2^{\text{Ph}}_{\text{PPh}_3}$ (Table S6, entries 1–4). At the same time, the overall MMA content of the polymer composition formed was 40% (mol % MMA-based repeat units) after 5 min, increased to 56% after 10 min, and finally decreased to 46% after 120 min. This implies that the free radical polymerization is mainly active during the reaction period, when a high concentration of active species of the ethylene polymerization is also present in the reaction mixture (for further discussion, see [Supporting Information](#)). At first sight, this indicates an interaction of both polymerization modes.

Microstructure Analysis of the Polymers Formed in Simultaneous Ethylene and MMA Polymerizations. Multiple techniques, such as differential scanning calorimetry (DSC), size exclusion chromatography (SEC) and diffusion ordered NMR spectroscopy (DOSY) were used for characterization of the polymers formed by simultaneous ethylene and MMA polymerization to clearly identify the nature of the resulting polymer products.

NMR analysis showed that the tacticity of the PMMA obtained from polymerizations in the presence of ethylene is comparable to PMMA obtained from free radical MMA homopolymerizations (62–65% rr, Table S7, Figure S26). For PMMA obtained from polymerizations with $1^{\text{R}}_{\text{PPh}_3}$ (R = Me, Ph) at high ethylene pressures (100 bar, 15 mol % MMA, Figure S27, green), the T_g of PMMA overlaps with the intensive melting endotherm for PE at a T_m of about 120 °C. Therefore, the T_g of PMMA was not observable. For experiments at lower ethylene pressures, PEs degree of branching (ca. 25/1000 C atoms, see Table S7) and the

MMA content (33 mol % at 50 bar, 58 mol % at 25 bar) increased, resulting in separate observable melting and glass transitions of PE (ca. 110 °C) and PMMA (ca. 124 °C), respectively, in the DSC traces (Figure S27). T_m and T_g are in the range of homo-PE and -PMMA, respectively. This indicates that either homopolymer mixtures or block copolymers, containing long block segments derived from ethylene or MMA, were formed.

However, in ^1H and $^{13}\text{C}\{^1\text{H}\}$ NMR spectra, no characteristic resonances for a transition between PE and PMMA blocks were detected, as would be expected for block copolymers.²⁷ Instead, detailed polymer analysis by extraction experiments, DOSY, and SEC strongly indicate that under the conditions applied ($1^{\text{Me}}_{\text{PPh}_3}$, or $2^{\text{R}}_{\text{PPh}_3}$ with R = Me, Ph, 70 °C, 25 bar of ethylene, neat MMA, 15 μmol of [Ni], and 3 equiv of PPh₃) homopolymer mixtures of PE and PMMA were formed (Figure 3, Figure S30–S34).

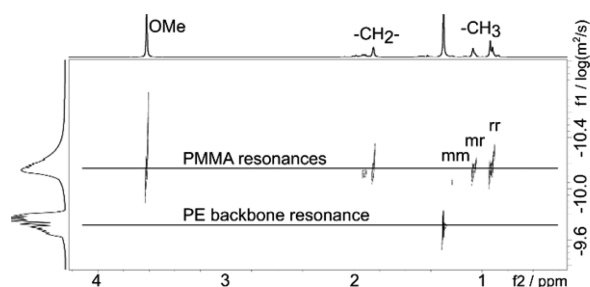


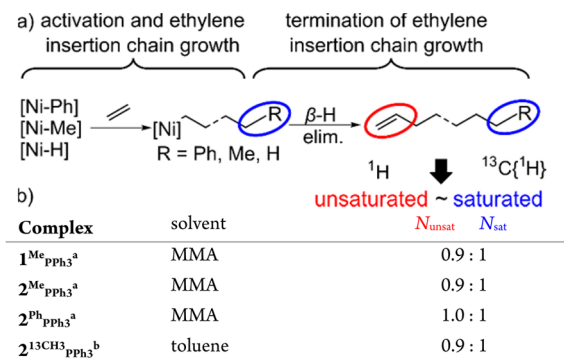
Figure 3. ^1H DOSY (600 MHz, 130 °C, 1,1,2,2-tetrachloroethane- d_2) of a polymer mixture (52 mol % MMA-based repeat units) polymerized with $1^{\text{Me}}_{\text{PPh}_3}$, plus 3 equiv of PPh₃ in 50 mL of MMA, 25 bar of E, 70 °C, and 30 min reaction time. PMMA resonances ($D = 7.8 \times 10^{-10} \text{ m}^2 \cdot \text{s}^{-1}$) and PE backbone resonance ($D = 2.0 \times 10^{-10} \text{ m}^2 \cdot \text{s}^{-1}$) show separate diffusion traces.

Molecular weights estimated by SEC (40 °C, THF, vs PS standards) of the PE fractions are in the range of 3000–6000 $\text{g} \cdot \text{mol}^{-1}$ ($M_w/M_n \approx 1.2\text{--}1.3$) and 60000–110000 $\text{g} \cdot \text{mol}^{-1}$ ($M_w/M_n \approx 2\text{--}3$) of the PMMA fractions. Similar values are expected for polymers obtained from polymerizations of each monomer alone under comparable conditions.

In addition, detailed NMR studies showed that the relative amount of saturated end groups per PE chain (N_{sat} , normalized to 1 group per PE chain) introduced upon the start of a new chain in insertion chain growth are almost equal to the relative amount of unsaturated chain ends (N_{unsat}) formed via $\beta\text{-H}$ elimination (Scheme 1). This suggests that the PE chain growth starts by insertion of ethylene into [Ni–Me]/[Ni–Ph] catalyst precursors or intermediate [Ni–H] species and is terminated by $\beta\text{-H}$ elimination, without any impact of MMA. In agreement, the same ratio of N_{unsat} to N_{sat} is obtained in the absence of MMA (Scheme 1b, entries 1–3 vs 4). This suggests that the insertion chain growth species [Ni–PE] does not participate in the generation of free radicals and is not impacted by the growing PMMA radicals, because this would result in a significantly different ratio of unsaturated and saturated end groups.

In summary, the key reaction steps of the insertion polymerization of ethylene (activation, chain growth, and termination) seem to proceed without interaction of the simultaneous free radical MMA polymerization. Both ethylene insertion and radical polymerization run simultaneously and are not influenced by each other. However, it was shown that the generation of free radicals is more feasible in the presence of ethylene, in comparison to

Scheme 1. (a) Schematic Representation of the Activation and Termination of the Ethylene Insertion Chain Growth and (b) Observed Relative Amounts of Unsaturated (N_{unsat}) and Saturated (N_{sat}) End Groups per PE Chain^c

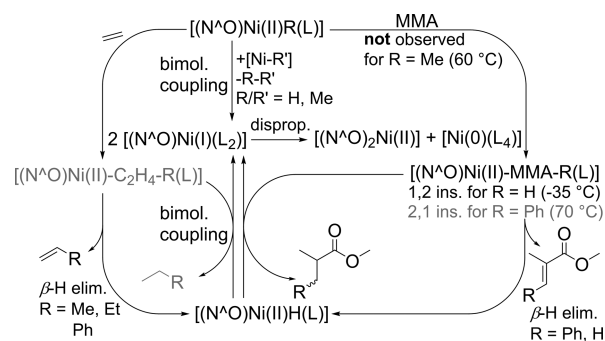


^aArithmetic mean for polymerizations stopped after 5, 10, 30, 60, and 120 min. ^bPolymerization time of 10 min. ^cReaction conditions: solvent volume = 50 mL, 25 bar of E, 15 μmol of [Ni], 3 equiv of PPh₃, 70 °C. Details see Supporting Information.

polymerizations of MMA alone. Therefore, we anticipate that reaction products of catalyst precursors are involved in the initiation of the free radical polymerization.

Stoichiometric Reactivity of Ethylene and MMA toward (N^ΛO)Ni(II)-Catalyst Precursors and Intermediate Ni Species. To identify the aforementioned Ni species, reactions of ethylene and MMA with Ni species that are anticipated to be involved in the polymerization process were monitored by spectroscopic methods (Scheme 2, NMR and EPR; detailed description, see Supporting Information).

Scheme 2. Summarized Reactivity of [(N^ΛO)Ni(II)R(L)] Catalyst Precursors and Intermediate Ni Species as Derived from Stoichiometric Experiments^a



^aFor details, see Supporting Information. Gray structures were not directly observed.

[Ni–Ph] complexes ($1^{\text{Ph}}_{\text{PPh}_3}$, $2^{\text{Ph}}_{\text{PPh}_3}$, and $3^{\text{Ph}}_{\text{PPh}_3}$) inserted MMA in a 2,1 fashion at 70 °C, followed by a rapid $\beta\text{-H}$ elimination. [Ni–Me] complexes showed no reactivity toward MMA under the conditions applied ($1^{\text{Me}}_{\text{DMSO}}$ and $1^{\text{Me}}_{\text{PPh}_3}$, 60 °C). This agrees with the observed undisturbed ethylene polymerization in the presence of MMA (vide supra). Therefore, it is concluded that [Ni–alkyl] complexes do not insert MMA. Reactive [Ni–H] complex, $1^{\text{H}}_{\text{PMe}_3}$, which is formed via $\beta\text{-H}$ elimination from [Ni–alkyl] complexes after ethylene or MMA insertion into the catalyst precursors, is readily able to reversibly insert MMA in a

1,2 fashion at low temperatures ($-35\text{ }^{\circ}\text{C}$, THF- d_8), while at higher temperatures (greater than $-2\text{ }^{\circ}\text{C}$), β -H elimination as the reverse reaction is favored. Kinetic studies revealed that the second order rates for the insertion of MMA and ethylene¹⁵ into intermediate $[\text{Ni}-\text{H}]$ species are on a similar order and can compete under polymerization conditions. No consecutive insertions of MMA were observed. This was accounted for by a fast β -H elimination in comparison to a second insertion of MMA into $[\text{Ni}-\text{alkyl}]$ complexes.

The stoichiometric experiments also provide insights into decomposition pathways: Reductive elimination of methyl moieties to the labile phosphine ligand (PPh_3) led to methyl phosphonium salt formation. Furthermore, reductive elimination from intermediately formed $[\text{Ni}-\text{H}]$ species to the $\text{N}^{\wedge}\text{O}$ ligand was observed. Previously, similar decomposition reactions for other $[\text{Ni}-\text{H}]$ species were described by Jenkins and Brookhart²⁸ and Grubbs et al.¹⁴ In both reductive elimination pathways, $\text{Ni}(0)$ species are expected to be formed. In addition, decomposition via bimolecular reductive coupling was observed, which proceeded even under mild conditions in the presence of $[\text{Ni}-\text{H}]$ species, or under more harsh conditions from catalyst precursor complexes (ethane formation from $[\text{Ni}-\text{Me}]$). Herein, we conclude from observed reactivities, that two Ni complexes, $[\text{Ni}(\text{II})-\text{R}]$ and $[\text{Ni}(\text{II})-\text{R}']$, react to form two intermediate $[\text{Ni}(\text{I})]$ species and release the coupled product $\text{R}-\text{R}'$ (Scheme 2, center). This intermediate species was directly observed in a reaction mixture of $[(\text{N}^{\wedge}\text{O})_{i\text{Pr},t\text{Bu-H}}\text{NiPh}(\text{PPh}_3)]$ and ethylene by spectroscopic methods (Figure 4, right).

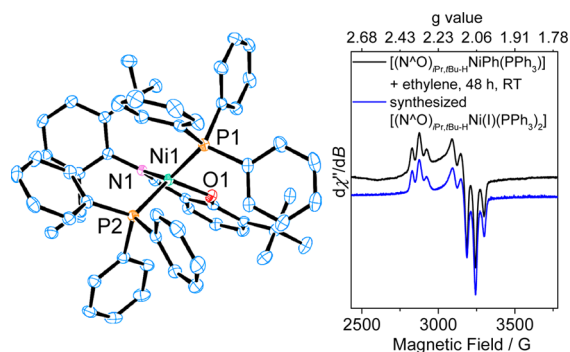


Figure 4. Identification of the paramagnetic $[\text{Ni}(\text{I})]$ complex $[(\text{N}^{\wedge}\text{O})_{i\text{Pr},t\text{Bu-H}}\text{Ni}(\text{I})(\text{PPh}_3)_2]$ formed during the reaction of $3\text{PPh}_3^{\text{Ph}}$ with ethylene. ORTEP (50% probability ellipsoids, hydrogens are omitted for clarity) plot determined by X-ray diffraction is shown left, and X band EPR spectra (9.36 GHz, toluene, $-170\text{ }^{\circ}\text{C}$) of the reaction mixture of $3\text{PPh}_3^{\text{Ph}}$ (27 mM) and 9 equiv of ethylene after 48 h at room temperature (black) and of separately synthesized $3\text{PPh}_3^{\text{Ph}}$ (blue) on the right.

The corresponding $[\text{Ni}(\text{I})]$ species, $[(\text{N}^{\wedge}\text{O})_{i\text{Pr},t\text{Bu-H}}\text{Ni}(\text{I})(\text{PPh}_3)_2]$, which was independently synthesized and characterized, represents the first isolated $[(\text{N}^{\wedge}\text{O})\text{Ni}(\text{I})]$ complex. This complex underwent further disproportionation to finally form a bis-chelated $[(\text{N}^{\wedge}\text{O})_2\text{Ni}(\text{II})]$ complex and the corresponding $[\text{Ni}(0)]$ species. In the presence of MMA and PPh_3 complex $[(\text{PPh}_3)_2\text{Ni}(0)(\eta^2\text{-H}_2\text{C}=\text{C}(\text{CH}_3)\text{COOMe})]$ was identified as a main $[\text{Ni}(0)]$ species (Figure S49–S51). These results give useful insights into possible reaction pathways and products that can be formed during the simultaneous ethylene and MMA polymerization. However, the source of organic free radicals still remains elusive at this point.

Sources of Organic Free Radicals in $(\text{N}^{\wedge}\text{O})\text{Ni}(\text{II})\text{R}(\text{L})$ Mediated Polymerizations.

We have elucidated that neither the organic moiety of the catalyst precursor nor the growing alkyl PE chain at the Ni center is involved in the initiation process of the free radical polymerization. Two possible initiation reactions for free radical polymerizations, which are supposed from an overall view of the observed reactivity, will be discussed in the following:

As a starting point, end group analysis of PMMA formed with $1_{\text{PPh}_3}^{\text{CH}_3}$ and PPh_3 revealed phenyl end groups instead of the anticipated methyl end groups and thus indicated the aryl phosphine as a source of initiating organic radicals (Figure 1). Also, additional phosphine was shown to have a crucial impact on the efficiency of the radical polymerization (vide supra). Tertiary phosphines are widely used as labile ligands and are often employed in homogeneous catalysis. They are usually considered to remain intact during catalysis; however, a number of examples have been reported where this is not the case.²⁹ Various pathways for a transfer of an aryl group from $\text{P}(\text{aryl})_3$ to the PMMA formed are conceivable, and we propose a homolytic $\text{P}-\text{C}$ bond cleavage as the most plausible pathway (additional pathways are discussed in the Supporting Information).

Photodriven $\text{P}-\text{C}$ bond cleavage was reported for PPh_3 ,³⁰ and tri-*o*-tolylphosphine was even described as a rapid free radical photopolymerization initiator.³¹ Ru mediated homolytic cleavage of a $\text{P}-\text{C}$ bond driven by light was reported recently and used for the initiation of a free radical polymerization of MMA.³² A thermal $\text{P}-\text{C}$ bond cleavage is considered, since all polymerizations were conducted under exclusion of light. Thermal Li-mediated homolytic $\text{P}-\text{C}$ bond cleavages are known for $\text{P}-\text{aryl}$ and $\text{P}-\text{alkyl}$ bonds, and mechanistic studies indicate that prior to the $\text{P}-\text{C}$ bond cleavage the metal is oxidized (Li^0 to Li^+) and the phosphine is reduced.³³ A similar reactivity for $\text{Cr}(0)$ complexes has been explored by computational methods by Espinosa et al.³⁴ A reduction of PPh_3 by Ni species requires a ready oxidation of these metal species. Therefore, we investigated the efficiency of low-valent $\text{Ni}(0/\text{I})$ species, which can form during polymerization, to initiate free radical polymerizations in the presence of phosphines. However, MMA homopolymerizations initiated with $[\text{Ni}(0)(\text{PPh}_3)_4]$ did not result in the formation of Ph end groups and an induction period was observed, which was not the case when $[(\text{N}^{\wedge}\text{O})\text{Ni}(\text{II})\text{R}(\text{PPh}_3)]$ complexes were employed as initiators (Figure S65 vs Figure S16). Also, $[(\text{N}^{\wedge}\text{O})_{i\text{Pr},t\text{Bu-H}}\text{Ni}(\text{I})(\text{PPh}_3)_2]$ did not efficiently initiate a radical polymerization ($16.3\text{ mmol}\cdot\text{L}^{-1}$ of $[\text{Ni}]$, neat MMA, $70\text{ }^{\circ}\text{C}$, 1 h, Table S9, entry 6). It can be concluded, that low-valent Ni species are not involved in the homolytic $\text{P}-\text{C}$ bond cleavage.

To elucidate the nature of the initial free radical more directly, spin trapping experiments were performed with $1_{\text{DMSO}}^{\text{Me}}$, an excess of PPh_3 , and α -phenyl-*N*-*tert*-butylnitrone (PBN) at $70\text{ }^{\circ}\text{C}$ in toluene (Figure 5, top). After 18 h a distinct EPR resonance of a nitrosyl radical was detected. Comparison with separately synthesized Me- and Ph-PBN spin adducts³⁵ indicates that the phenyl spin adduct was formed (Figure S61 and S62). The phosphine free system, $1_{\text{DMSO}}^{\text{Me}}$, under otherwise identical conditions led to formation of a different, unassigned PBN spin adduct (Figure S64). In summary, we believe this pathway is the most likely and propose a thermal metal-mediated homolytic $\text{P}-\text{C}$ bond cleavage for aryl phosphine ligands in $[(\text{N}^{\wedge}\text{O})\text{Ni}(\text{II})\text{R}(\text{PAr}_3)]$ complexes.

A second possible pathway to initiate a free radical polymerization of MMA is indicated by a higher efficiency of $(\text{N}^{\wedge}\text{O})\text{Ni}$ complexes with iodo substituted $\text{N}^{\wedge}\text{O}$ ligands ($1_{\text{PPh}_3}^{\text{Ph}}$ and $2_{\text{PPh}_3}^{\text{Ph}}$) in comparison to iodo free complexes ($3_{\text{PPh}_3}^{\text{Ph}}$, Tables 1

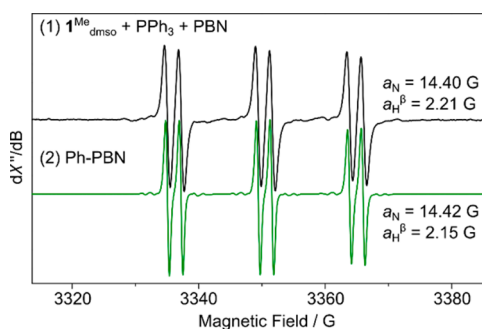


Figure 5. CW X-band (9.37 MHz, RT) EPR spectra of the trapped radical of the reaction of $1^{\text{Me}}_{\text{DMSO}}$ (4 mM) with 4 equiv of PPh_3 and 13 equiv of PBN at 70 °C after 18 h in toluene (1) and of the separately synthesized phenyl PBN spin adduct (2).

and 2). A significant discrepancy was also noticed in stoichiometric NMR experiments. Observing the reactivity of $[(\text{N}^{\bullet}\text{O})_{\text{IPr,tBu-H}}\text{Ni(II)Ph}(\text{PPh}_3)]$ toward MMA ultimately led to formation of $[(\text{N}^{\bullet}\text{O})_{\text{IPr,tBu-H}}\text{Ni(II)}]$ and $[(\text{PPh}_3)_2\text{Ni(0)}\eta^2\text{-MMA}]$ (vide supra, Figure S49). In contrast, during NMR experiments with iodo substituted $\text{N}^{\bullet}\text{O}$ ligands (1 and 2), no $[\text{Ni(0)}]$ species could be detected, although various decomposition pathways should lead to the formation of $[\text{Ni(0)}]$ species. Therefore, the reactivity of Ar-I functionalities and $[\text{Ni(0)}]$ species was examined more closely. Tsou and Kochi³⁶ found that the oxidative addition of aryl halides to $[\text{Ni(0)}]$ can be separated into two distinct one electron transfer steps. In the first step, the aryl halide is reduced. In the following step, either the oxidative addition product $[(\text{L})_n\text{Ni(II)X(Ar)}]$ is formed or an aryl radical escapes the solvation sphere and $[(\text{L})_n\text{Ni(I)X}]$ is formed along with an organic free radical. Free radical polymerizations initiated by low-valent Ni species and organic halides are also known.³⁷ Indeed, $[\text{Ni(0)}(\text{PPh}_3)_4]$ with addition of iodo aryls effectively initiated a radical polymerization of MMA (neat MMA, 70 °C, 0.5 $\text{mmol}\cdot\text{L}^{-1}$, 64 equiv of PhI, 1.2 chains/ $[\text{Ni}]$, 5 h, Table S9, entry 2). $[(\text{PPh}_3)_3\text{Ni(I)Cl}]$ showed a similar reactivity (neat MMA, 70 °C, 1.1 $\text{mmol}\cdot\text{L}^{-1}$, 33 equiv of PhI, 1.5 chains/ $[\text{Ni}]$, 7 h, Table S9, entry 5) under comparable reaction conditions. These results clearly show that isolated low-valent Ni(0/I) species effectively initiate free radical MMA polymerizations in the presence of Ar-I functionalities. To verify whether this pathway is also accessible from $[(\text{N}^{\bullet}\text{O})\text{Ni(II)R(L)}]$ systems, 40 equiv of PhI was added to a polymerization mixture of iodo free Ni(II) salicylaldiminato complex $[(\text{N}^{\bullet}\text{O})_{\text{CF, Ant-H}}\text{NiMe}(\text{pyridine})]$ (4 equiv of PPh_3 and neat MMA). Indeed, increased conversions from ca. 3% to 5% were observed (70 °C, $c([\text{Ni}]) = 0.5 \text{ mmol}\cdot\text{L}^{-1}$, 5 h, Figure S67). Hence, it seems likely that the *in situ* generated low-valent Ni-species together with iodo substituted $\text{N}^{\bullet}\text{O}$ ligands contribute to the formation of organic free radicals. According to MALDI-TOF MS and NMR analysis, no end groups were transferred to the formed PMMA polymer by this initiation pathway and the formed end group is independent of Ar and X (Figure S66, red = 3,5-dimethoxy-bromobenzene and black = $(\text{N}^{\bullet}\text{O})_{\text{IPr,tBu-H}}$ as Ar-X). We believe, that the intermediate radical formation proceeds in the ligand sphere of $[(\text{PPh}_3)_2\text{Ni}(\eta^2\text{-H}_2\text{C}=\text{C}(\text{CH}_3)\text{COOMe})]$ (vide supra), and here, for example, a hydrogen abstraction from the $\alpha\text{-CH}_3$ group of MMA³⁸ is more likely than the addition of the organic radical to the double bond of MMA.

In summary, the major initiation reaction for radical polymerizations in the $(\text{N}^{\bullet}\text{O})\text{Ni(II)R}(\text{P}(\text{aryl})_3)$ systems studied in the simultaneous ethylene and MMA polymerization is the

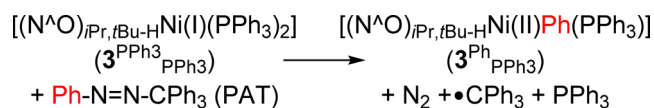
reaction of $[\text{Ni(0)}]/[\text{Ni(I)}]$ with iodo substituted $\text{N}^{\bullet}\text{O}$ ligands (1 and 2). This is a rather specific case, because these ligands are not widely used; however $2^{\text{Ph}}_{\text{PPh}_3}$ was the subject of a previous study on a dual radical/insertion polymerization.²⁰ A possible P–C bond cleavage in aryl phosphine ligands as an organic radical releasing reaction is a somewhat more general pathway since phosphines are widely used in organometallic catalytic systems.

Two possible pathways for the initiation of a free radical polymerization were suggested; however, we want to emphasize that these do not represent the only possible pathways for an initiation of a radical polymerization. For example, iodine and phosphine free systems were also found to be able to initiate radical polymerizations ($[(\text{N}^{\bullet}\text{O})_{\text{CF, Ant-H}}\text{NiMe}(\text{pyridine})]$, Figure S67, red). These further pathways were not subject of the present study.

Reactivity of Ni(I) toward Organic Radicals. Although the intermediately formed $[(\text{N}^{\bullet}\text{O})\text{Ni(I)}]$ species do not initiate free radical polymerizations, their reactivity toward organic radicals is of interest, since metal centered radicals are reactive species in controlled radical polymerizations.²⁴

Upon reaction of $[(\text{N}^{\bullet}\text{O})_{\text{IPr,tBu-H}}\text{Ni(I)}(\text{PPh}_3)_2]$ ($3^{\text{PPh}_3}_{\text{PPh}_3}$) with 15 equiv of phenylazo-triphenylmethane (PAT, Scheme 3), an

Scheme 3. Combination of Organic and Metal Centered Radical Species



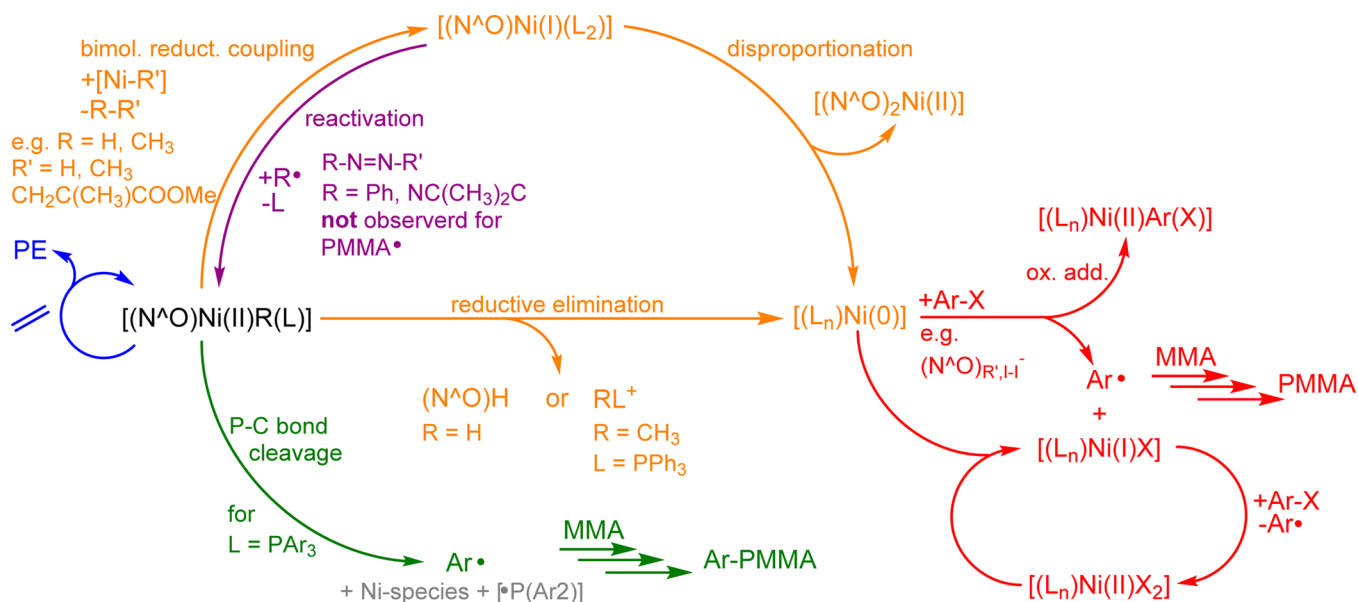
immediate formation of $[(\text{N}^{\bullet}\text{O})_{\text{IPr,tBu-H}}\text{Ni(II)Ph}(\text{PPh}_3)]$ and noncoordinated PPh_3 was observed by NMR spectroscopy (RT, C_6D_6 , Figures S68 and S69). $3^{\text{PPh}_3}_{\text{PPh}_3}$ also reacted rapidly with AIBN; however, no $[\text{Ni-alkyl}]$ species could be identified, which was accounted for by rapid $\beta\text{-H}$ elimination. These reactions were much faster than the expected thermally induced decomposition of PAT³⁹ or AIBN⁴⁰ to free radicals, and therefore the reaction seems to be metal mediated. We hypothesized that this observed reactivity can be used to capture intermediate $[\text{Ni(I)}]$ complexes, formed via bimolecular reductive coupling, to reestablish a catalytically active species directly in the insertion polymerization mixture by the addition of a free radical source (e.g., azo compounds) to prevent further decomposition.

As a proof of principle, we carried out polymerizations of ethylene in the presence of azo compounds with complex $2^{\text{Ph}}_{\text{PPh}_3}$ (Table 3). Addition of TAP or AIBN led to a significant

Table 3. Ethylene Polymerizations with Catalyst Precursor $2^{\text{Ph}}_{\text{PPh}_3}$, with or without Addition of Azo Compounds at 25 °C^a

entry	equiv add.	yield, g	lifetime, ^b min	TOF ^c	T_m , ^d °C
1	0	0.92	30	8750	132
2	2 PAT	1.87	50	10670	132
3	2 AIBN	2.28	60	10840	132
4	4 AIBN	5.77	>180	9140	132
5	6 AIBN	6.57	>190	9860	132

^aReaction conditions: 100 mL of toluene, 7.5 μmol of $[\text{Ni}]$, 25 bar of E, 25 °C. ^bLifetime is determined when no further consumption of ethylene is detected by mass flow meter. ^c $n(\text{E})\cdot n([\text{Ni}])^{-1}\cdot\text{h}^{-1}$. ^dDetermined by DSC.

Scheme 4. Schematic Overview of the Reactivity of $[(N^{\wedge}O)Ni(II)R(L)]$ Complexes in the Presence of Monomers (Ethylene and MMA)^a

^aDifferent pathways are color-coded. Blue describes migratory insertion polymerization, orange describes formation of $[Ni(I)]$ and $[Ni(0)]$ species, green describes homolytic P–C bond cleavage, red describes one electron oxidation of $[Ni(0/I)]$ species, and purple describes formation of $[Ni(II)(alkyl/aryl)]$ from $Ni(I)$ species.

increase in yield and lifetime in the ethylene polymerization. The lifetime increased from 30 to >190 min in case of 0 or 6 equiv of AIBN added (Table 3, entry 1 vs 5). At the same time, the turnover frequencies (TOF) and the microstructure of the resulting PE polymers (concluded from T_m) remained unchanged, indicating that the same active species was present in the reaction mixtures (for a detailed discussion, see Supporting Information).

In summary, $[(N^{\wedge}O)Ni(I)]$ species that are formed during the polymerization via bimolecular reductive coupling can be transformed into the corresponding catalytically active $[(N^{\wedge}O)Ni(II)R]$ species by reaction with organic radicals.

CONCLUDING REMARKS

To date, reported observations of the reactivity of MMA in $Ni(II)$ -catalyzed polymerizations provided an inconclusive picture. To elucidate the role of free radicals in these reactions, we have performed (a) synthesis of different $(N^{\wedge}O)Ni(II)R(L)$ catalyst precursors ($R = Ph, Me$), intermediate species, and decomposition products, (b) homopolymerizations of MMA and polymerizations of ethylene in the presence of MMA, (c) detailed analysis of the polymers formed (labeling experiments, end group analysis, microstructure analysis), and (d) stoichiometric experiments monitored via spectroscopic methods (NMR and EPR). Combining these methods, the following picture emerged (Scheme 4). (1) The migratory insertion polymerization of ethylene (Scheme 4, blue) is virtually unaffected by a simultaneous radical polymerization of MMA. Ethylene chain growth is initiated by insertion of ethylene into $[Ni-Me]/[Ni-Ph]$ catalyst precursors or into intermediately formed $[Ni-H]$ species and is mainly terminated by β -H elimination (conclusive with end group analysis). The growing $[Ni-polymer]$ species is not relevant for the formation of free radicals that initiate the radical chain growth of MMA. Furthermore, no interaction of insertion and radical polymer-

ization was observed, resulting in homopolymer mixtures of PE and PMMA. However, the presence of MMA led to decreased productivities in the ethylene polymerizations, which is accounted for by an inhibition of insertion polymerization by MMA as a weakly coordinating solvent. (2) Concerning the reactivity of $[(N^{\wedge}O)Ni(II)R(L)]$ precursors ($R = Me, Ph$) and active species ($R = H$) toward MMA, it was found that $[Ni-H]$ (1,2 insertion mode) and $[Ni-Ph]$ (2,1 insertion mode) complexes insert MMA to form thermally unstable $[Ni-alkyl]$ complexes. These undergo rapid β -H eliminations instead of a further insertion of monomer species, which is believed to be suppressed by chelate formation by coordination of the inserted monomers' carbonyl group.^{14–16} Interestingly, $[Ni-Me]$ catalyst precursors, which are also a model for the growing PE chain, did not insert MMA under the conditions applied. Instead, these complexes undergo decomposition by either reductive elimination to the labile phosphine ligand (to form $MePPh_3^+$) or bimolecular reductive coupling with formation of ethane (Scheme 4, orange). In addition, supplying ^{13}C labeled $[Ni-^{13}CH_3]$ as an initiator in MMA homopolymerizations did not lead to an incorporation of the labeled group into the PMMA polymer chain. $[Ni-Me]$ and $[Ni-Ph]$ complexes showed very similar kinetic behavior for MMA homopolymerizations, indicating that an insertion of MMA into the $Ni-C$ bond is not a mandatory reaction in the generation of radicals that initiate MMA free radical chain growth. (3) As one source for organic free radicals, we suggest a homolytic P–C bond cleavage in labile aryl phosphine ligands (Scheme 4, green). Phenyl terminated PMMA polymers were formed when the radical polymerization was initiated with $[(N^{\wedge}O)_{CF_3I}Ni(^{13}CH_3)PPh_3]$ and 3 equiv of PPh_3 . The sole possible phenyl source herein is PPh_3 . By variation of the phosphine ligand to $P(mTol)_3$, a variation of the polymer end group pattern in the 1H NMR spectrum was observed. In addition, spin trapping EPR experiments have shown that $I_{PPh_3}^{Me}$ with PBN led to the $Ph-PBN$ spin adduct (Figure 5). Although this aspect was not studied in detail, we

believe the P–C bond cleavage is metal-mediated and occurs from the initial $[(N^{\wedge}O)Ni(II)R(PPh_3)]$ complex. Also, P–C bond cleavage could be an explanation for higher efficiency for radical polymerizations with $[Ni]$ complexes when additional phosphine is added, which was reported repeatedly previously^{20,41} and was also observed in our experiments. (4) A second radical source, much more specific to the nickel complexes under investigation, is one electron oxidation/single electron transfer from intermediately formed $[Ni(0)]$ species to aryl halides, for example, the aryl iodide moiety of the $N^{\wedge}O$ ligand, whereby metal-centered $Ni(I)$ and ligand-based aryl radicals are formed (Scheme 4, red). (5) With respect to the generation of $[Ni(0)]$ species, we have identified several reaction pathways: (a) reductive elimination of $(N^{\wedge}O)H$ from $(N^{\wedge}O)Ni$ hydride complexes formed during chain transfer in the ethylene polymerization; (b) reductive elimination of $MeP(aryl)_3^+$ from $(N^{\wedge}O)Ni$ methyl phosphine complexes; (c) a relevant alternative pathway, especially at high $[Ni]$ concentrations as present in NMR experiments, is a bimolecular reductive coupling ($[Ni-R] + [Ni-R'] \rightarrow R-R' + 2 [Ni(I)]$). We have studied this reaction in detail for $[Ni-H]$ species (Scheme 4, orange top pathway) and identified the intermediate formation of $[(N^{\wedge}O)Ni(I)(PPh_3)_2]$, which underwent a further disproportionation reaction ultimately leading to the observed formation of $[(N^{\wedge}O)_2Ni(II)]$ and $[Ni(0)(PPh_3)_4]$. This pathway can proceed under mild conditions with involvement of $[Ni-H]$ species and is believed to proceed in a similar manner under more harsh conditions also for $[Ni-Me]$ and $[Ni-Ph]$ complexes. In simultaneous polymerizations of ethylene and MMA, the initiation process was found to be significantly faster than in polymerizations of MMA alone. This is traced to a fast ethylene insertion into the catalyst precursors, which yields $[Ni-alkyl]$ complexes. These readily undergo β -H elimination, and reactive $[Ni-H]$ species form, which decompose by bimolecular reductive coupling and finally form $[Ni(0)]$ species. These $[Ni(0)]$ species react with aryl halide functionalities in the specific $N^{\wedge}O$ ligands and initiate a free radical chain growth. (6) Intermediately formed $[Ni(I)]$ species may be transformed into insertion polymerization active $Ni(II)$ (aryl/alkyl) prior to disproportionation into $Ni(0)$ complexes and polymerization inactive bis(chelate) nickel(II) by addition of azo-compounds (Scheme 4, purple). By using this strategy, the overall productivity of an exemplified catalyst studied here has been increased by a factor of 6 in ethylene polymerizations due to regeneration of insertion polymerization active species. It has to be emphasized that an analogous recombination of $[Ni(I)]$ species with growing PMMA radicals cannot be excluded. However, since the insertion products of MMA into $[Ni-H]$ and $[Ni-Ph]$ undergo rapid β -hydride elimination rather than ethylene insertion, the formation of PMMA–PE block copolymers is precluded.

■ ASSOCIATED CONTENT

Supporting Information

The Supporting Information is available free of charge on the ACS Publications website at DOI: 10.1021/jacs.5b08612.

Structure of $1^{Ph}_{PPh_3}$ (CCDC Number: 1432837) (CIF)

Structure of $2^{Ph}_{PPh_3}$ (CCDC Number: 1432838) (CIF)

Structure of {3-3} (CCDC Number: 1432839) (CIF)

Structure of $[(N^{\wedge}O)_{iPr,tBu-H}Ni(\mu^2-OH)_2Ni(N^{\wedge}O)_{iPr,tBu-H}]$ (CCDC Number: 1432840) (CIF)

Structure of 3^{PPh_3} (CCDC Number: 1432842) (CIF)

Structure of $3^{Ph}_{PPh_3}$ (CCDC Number: 1432841) (CIF)

Synthetic procedures, characterizations of complexes, spectroscopic data for key experiments, and experimental and calculation details (PDF)

■ AUTHOR INFORMATION

Corresponding Author

*E-mail: stefan.mecking@uni-konstanz.de.

Notes

The authors declare no competing financial interest.

■ ACKNOWLEDGMENTS

This work was financially supported by the DFG (Grant Me 1388/10-2). The authors thank Michael Gießl and Julia Zimmerer for performing pressure reactor experiments, Anke Friemel and Ullrich Haunz for technical assistance with NMR measurements, Lars Bolk for DSC and SEC measurements, and Evelyn Wuttke for technical support with EPR measurements.

■ REFERENCES

- (1) Nakamura, A.; Ito, S.; Nozaki, K. *Chem. Rev.* **2009**, *109*, 5215–44.
- (2) (a) Johnson, L. K.; Mecking, S.; Brookhart, M. *J. Am. Chem. Soc.* **1996**, *118*, 267–8. (b) Mecking, S.; Johnson, L. K.; Wang, L.; Brookhart, M. *J. Am. Chem. Soc.* **1998**, *120*, 888–99.
- (3) Drent, E.; van Dijk, R.; van Ginkel, R.; van Oort, B.; Pugh, R. I. *Chem. Commun.* **2002**, 744–5.
- (4) Nakamura, A.; Anselment, T. M. J.; Claverie, J.; Goodall, B.; Jordan, R. F.; Mecking, S.; Rieger, B.; Sen, A.; van Leeuwen, P. W. N. M.; Nozaki, K. *Acc. Chem. Res.* **2013**, *46*, 1438–49.
- (5) Kochi, T.; Noda, S.; Yoshimura, K.; Nozaki, K. *J. Am. Chem. Soc.* **2007**, *129*, 8948–9.
- (6) Ito, S.; Munakata, K.; Nakamura, A.; Nozaki, K. *J. Am. Chem. Soc.* **2009**, *131*, 14606–7.
- (7) Rünzi, T.; Fröhlich, D.; Mecking, S. *J. Am. Chem. Soc.* **2010**, *132*, 17690–1.
- (8) Guironnet, D.; Roesle, P.; Rünzi, T.; Göttker-Schnetmann, I.; Mecking, S. *J. Am. Chem. Soc.* **2009**, *131*, 422–3.
- (9) Rünzi, T.; Guironnet, D.; Göttker-Schnetmann, I.; Mecking, S. *J. Am. Chem. Soc.* **2010**, *132*, 16623–30.
- (10) (a) Wang, C. M.; Friedrich, S.; Younkin, T. R.; Li, R. T.; Grubbs, R. H.; Bansleben, D. A.; Day, M. W. *Organometallics* **1998**, *17*, 3149–51. (b) Johnson, L. K.; Bennett, A. M. A.; Ittel, S. D.; Wang, L.; Parthasarathy, A.; Hauptman, E.; Simpson, R. D.; Feldman, J.; Coughlin, E. B. (E. I. du Pont de Nemours & Co., USA) International Patent WO 98/30609, 1998.
- (11) (a) Zuideveld, M. A.; Wehrmann, P.; Röhr, C.; Mecking, S. *Angew. Chem.* **2004**, *116*, 887–91. (b) Tong, Q.; Krumova, M.; Göttker-Schnetmann, I.; Mecking, S. *Langmuir* **2008**, *24*, 2341–7. (c) Osichow, A.; Rabe, C.; Vogt, K.; Narayanan, T.; Harnau, L.; Drechsler, M.; Ballauff, M.; Mecking, S. *J. Am. Chem. Soc.* **2013**, *135*, 11645–50.
- (12) Younkin, T. R.; Connor, E. F.; Henderson, J. I.; Friedrich, S. K.; Grubbs, R. H.; Bansleben, D. A. *Science* **2000**, *287*, 460–2.
- (13) Connor, E. F.; Younkin, T. R.; Henderson, J. I.; Hwang, S.; Grubbs, R. H.; Roberts, W. P.; Litzau, J. J. *J. Polym. Sci., Part A: Polym. Chem.* **2002**, *40*, 2842–54.
- (14) Waltman, A. W.; Younkin, T. R.; Grubbs, R. H. *Organometallics* **2004**, *23*, 5121–3.
- (15) Berkefeld, A.; Drexler, M.; Möller, H. M.; Mecking, S. *J. Am. Chem. Soc.* **2009**, *131*, 12613–22.
- (16) Berkefeld, A.; Mecking, S. *J. Am. Chem. Soc.* **2009**, *131*, 1565–74.
- (17) He, X.; Wu, Q. *Appl. Organomet. Chem.* **2006**, *20*, 264–71.
- (18) Li, X.-F.; Li, Y.-G.; Li, Y.-S.; Chen, Y.-X.; Hu, N.-H. *Organometallics* **2005**, *24*, 2502–10.
- (19) (a) Rodriguez, B. A.; Delferro, M.; Marks, T. J. *J. Am. Chem. Soc.* **2009**, *131*, 5902–19. (b) Rodriguez, B. A.; Delferro, M.; Marks, T. J. *J. Am. Chem. Soc.* **2013**, *135*, 17651.

- (20) (a) Leblanc, A.; Grau, E.; Broyer, J.-P.; Boisson, C.; Spitz, R.; Monteil, V. *Macromolecules* **2011**, *44*, 3293–301. (b) Leblanc, A.; Broyer, J.-P.; Boisson, C.; Spitz, R.; Monteil, V. *Pure Appl. Chem.* **2012**, *84*, 2113–20.
- (21) (a) Carlini, C.; Martinelli, M.; Raspolli Galletti, A. M.; Sbrana, G. *J. Polym. Sci., Part A: Polym. Chem.* **2003**, *41*, 2117–24. (b) Carlini, C.; De Luise, V.; Martinelli, M.; Raspolli Galletti, A. M.; Sbrana, G. *J. Polym. Sci., Part A: Polym. Chem.* **2006**, *44*, 620–33.
- (22) (a) Göttker-Schnetmann, I.; Wehrmann, P.; Röhr, C.; Mecking, S. *Organometallics* **2007**, *26*, 2348–62. (b) Wehrmann, P.; Mecking, S. *Organometallics* **2008**, *27*, 1399–408.
- (23) (a) Bevington, J. C.; Melville, H. W.; Taylor, R. P. *J. Polym. Sci.* **1954**, *12*, 449–59. (b) Bevington, J. C.; Melville, H. W.; Taylor, R. P. *J. Polym. Sci.* **1954**, *14*, 463–76.
- (24) (a) Ouchi, M.; Terashima, T.; Sawamoto, M. *Chem. Rev.* **2009**, *109*, 4963–5050. (b) Poli, R. *Eur. J. Inorg. Chem.* **2011**, 1513–30.
- (25) Collins, S.; Ward, D. G. *J. Am. Chem. Soc.* **1992**, *114*, 5460–2.
- (26) (a) Hatada, K.; Kitayama, T.; Masuda, E. *Polym. J.* **1986**, *18*, 395–402. (b) Kashiwagi, T.; Inaba, A.; Brown, J. E.; Hatada, K.; Kitayama, T.; Masuda, E. *Macromolecules* **1986**, *19*, 2160–8.
- (27) Hiller, W.; Pasch, H.; Macko, T.; Hofmann, M.; Ganz, J.; Spraul, M.; Braumann, U.; Streck, R.; Mason, J.; Van Damme, F. *J. Magn. Reson.* **2006**, *183*, 290–302.
- (28) Jenkins, J. C.; Brookhart, M. *J. Am. Chem. Soc.* **2004**, *126*, 5827–42.
- (29) (a) Garrou, P. E. *Chem. Rev.* **1985**, *85*, 171–85. (b) Parkins, A. W. *Coord. Chem. Rev.* **2006**, *250*, 449–67. (c) Macgregor, S. A. *Chem. Soc. Rev.* **2007**, *36*, 67–76. (d) Albrecht, M. *Chem. Rev.* **2010**, *110*, 576–623. (e) Crabtree, R. H. *Chem. Rev.* **2015**, *115*, 127–50.
- (30) (a) Horner, L.; Dörger, J. *Tetrahedron Lett.* **1965**, *6*, 763–7. (b) Kaufman, M. L.; Griffin, C. E. *Tetrahedron Lett.* **1965**, *6*, 769–72. (c) Hwang, S. J.; Powers, D. C.; Maher, A. G.; Nocera, D. G. *Chem. Sci.* **2015**, *6*, 917–22.
- (31) Eldred, R. J. *J. Polym. Sci., Part A-1: Polym. Chem.* **1969**, *7*, 265–8.
- (32) Versace, D.-L.; Cerezo Bastida, J.; Lorenzini, C.; Cachet-Vivier, C.; Renard, E.; Langlois, V.; Malval, J.-P.; Fouassier, J.-P.; Lalevé, J. *Macromolecules* **2013**, *46*, 8808–15.
- (33) Dogan, J.; Schulte, J. B.; Swiegers, G. F.; Wild, S. B. *J. Org. Chem.* **2000**, *65*, 951–7.
- (34) Espinosa, A.; Gómez, C.; Streubel, R. *Inorg. Chem.* **2012**, *51*, 7250–6.
- (35) Kotake, Y.; Janzen, E. G. *J. Am. Chem. Soc.* **1988**, *110*, 3699–701.
- (36) Tsou, T. T.; Kochi, J. K. *J. Am. Chem. Soc.* **1979**, *101*, 6319–32.
- (37) (a) Uegaki, H.; Kamigaito, M.; Sawamoto, M. *J. Polym. Sci., Part A: Polym. Chem.* **1999**, *37*, 3003–9. (b) Grishin, D. F.; Valetova, N. B.; Il'ichev, I. S.; Prokhorova, M. G.; Beletskaya, I. P. *Russ. Chem. Bull.* **2006**, *55*, 2106–8. (c) Valetova, N. B.; Il'ichev, I. S.; Grishin, D. F. *Russ. J. Appl. Chem.* **2010**, *83*, 895–900.
- (38) Mavroudakos, E.; Cuccato, D.; Moscatelli, D. *J. Phys. Chem. A* **2014**, *118*, 1799–806.
- (39) Alder, M. G.; Leffler, J. E. *J. Am. Chem. Soc.* **1954**, *76*, 1425–7.
- (40) Sasaki, H.; Nagayama, M. *J. Appl. Polym. Sci.* **1967**, *11*, 2097–108.
- (41) Moineau, G.; Minet, M.; Dubois, P.; Teyssié, P.; Senninger, T.; Jérôme, R. *Macromolecules* **1999**, *32*, 27–35.